

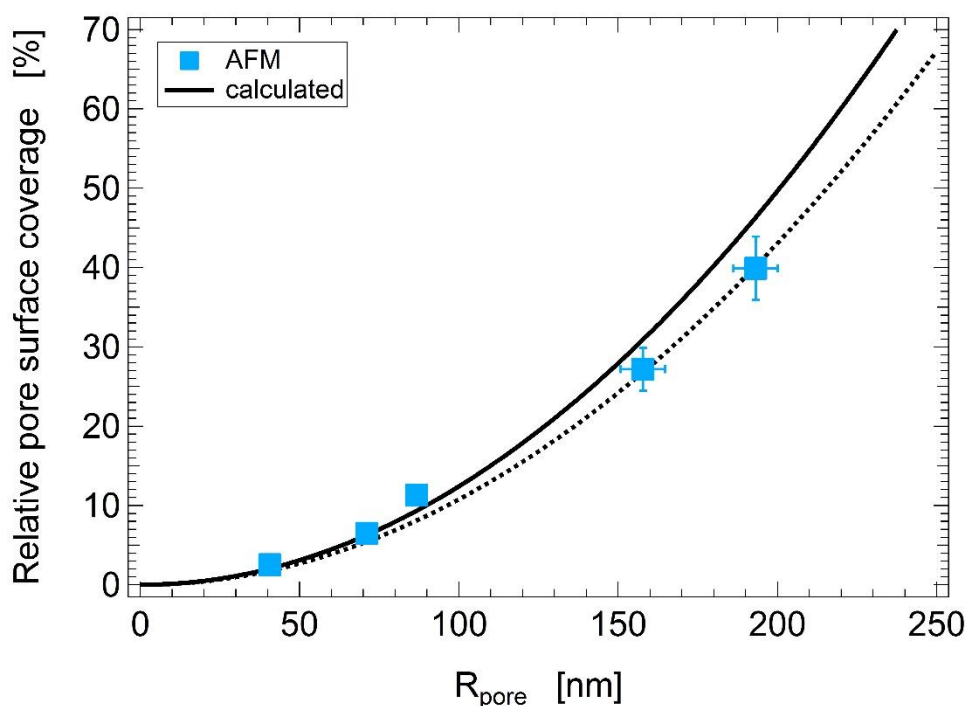
Electronic supplementary information

Oriented crystallization of PEG induced by confinement in cylindrical nanopores: Structural and thermal properties

Ann-Kathrin Grefe, Björn Kuttich, Lukas Stühn, Robert Stark and Bernd Stühn

Pore merging at high etching times

The AFM measurements discussed in section 3.1 show that for high etching times and thus large pore radii pores start to fuse. In order to quantify this effect, the relative pore surface coverage as observed via AFM is determined for the samples listed in table 1. Assuming the pores to be strictly straight and parallel to each other, this surface coverage corresponds to the porosity of the foils calculated in section 2.1.1. For each sample AFM images with a minimum of 100 pores are evaluated. The results are shown below in ESI fig. 1 as a function of pore radius. For comparison, the values calculated based on the pore density and the cylindrical pore form as described in section 2.1.1 are also included in ESI fig. 1 (solid line). Since a merging of pores results in a decrease of pore surface coverage, this should be reflected by a downward deviation of the values measured via AFM compared to the calculated ones.



ESI fig. 1 Relative pore surface coverage determined from AFM measurements as well as calculated as described in section 2.1.1 (solid line). The dashed line is a guide for the eye.

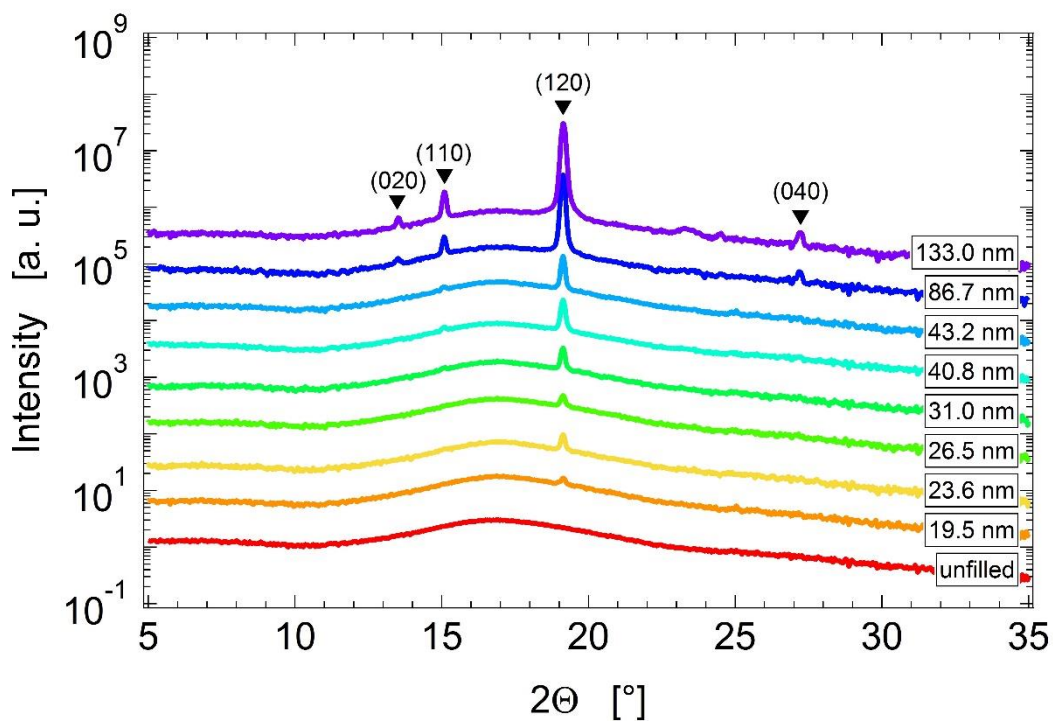
For pore radii up to about 90 nm the measured values agree well with the calculated ones, meaning that in this region no significant merging of pores is observed. Here the nanopores have a well-defined and uniform cylindrical shape. These findings are in accordance with the SAXS measurements discussed in section 3.1 (see fig. 2 and fig. 3), which show that up to a pore size of 133.0 nm pore radii can reliably be

determined from fits to the scattering curves with no increase in radius polydispersity being found. However, the larger pore sizes examined via AFM show a decrease (indicated by a dashed line) of the relative pore surface coverage compared to the calculated values. As presumed above, this loss of surface coverage is caused by the merging of pores at high etching times and large pore radii. For the largest pores used in the experiments a decrease of about 7 % is found. The low loss of surface coverage indicates that in most cases the pore merging is accounted for by marginal contact of pores, which retain most of their cylindrical shape. Larger, distorted clusters of pores only account for a small part of pore merging. However, even in these cases the strictly parallel orientation and high aspect ratio of the nanopores is not impaired. In conclusion, for all pore sizes examined in this work the ion track-etched polycarbonate constitutes a suitable one-dimensional confinement.

Wide angle X-ray scattering (WAXS)

WAXS scans were recorded using a D8 Advance reflectometer (Bruker AXS) in Θ/Θ geometry. A conventional X-ray tube (Bruker AXS) yields copper K_{α} radiation with $\lambda = 1.54 \text{ \AA}$. Details concerning beam monochromatization and focus can be found elsewhere.¹ The scattered intensity was measured over a 2Θ -range from 5° to 35° using a VÅNTEC-1 line detector (Bruker AXS) in continuous mode with a precision of 0.03° . Samples are placed on a sample stage in a distance of 30 cm from the detector, so that the sample surface is oriented perpendicularly to the plane of incidence. The sample stage background is subtracted from every scan.

ESI fig. 2 shows an overview over scattering curves of PEG filled nanopores of different radii together with an unfilled sample. All measurements were carried out below the melting point of PEG at a temperature of 30°C .



ESI fig. 2 Scattering curves of PEG filled samples of different pore radius as well as an unfilled sample measured at a temperature of 30°C . Curves are shifted vertically for clarity.

All scattering curves contain a broad shoulder around $2\theta = 17^\circ$. A comparison with the scan of an unfilled sample shows this shoulder to be a feature of the coated nanopores, most likely due to the amorphous SiO_2 shell. Therefore it is not considered further. For the largest examined pore radius of 133.0 nm four peaks can be identified at 2θ angles of 13.5° , 15.1° , 19.1° and 27.2° . These peaks can be assigned to the (020), (110), (120) and (040) reflections of the well-known monoclinic unit cell of bulk PEG with the corresponding parameters $a = 8.05 \text{ \AA}$, $b = 13.04 \text{ \AA}$, $c = 19.48 \text{ \AA}$ and $\beta = 125.4^\circ$.² As one can see, for the PEG confined in the nanopores only ($hk0$) reflections appear, which indicates the c -axis and thus the chain axis being oriented parallel to the sample surface and perpendicular to the pore axis. These findings are consistent with the conclusions drawn from SAXS measurements discussed in section 3.2.1. With decreasing pore size the heights of the observed peaks decline due to the reduced PEG sample volume. The prevailing (120) reflection can be distinguished down to the smallest examined pore radius of 19.5 nm, confirming the presence of crystalline structures even at such small pore sizes. No shift of peak positions can be seen, indicating that the dimensions of the PEG unit cell remain unvaried for all pore sizes. Furthermore, since with decreasing pore size no additional peaks appear in the scattering curves (in particular the high intensity (032) reflection at 23.3° is not observed), the crystalline orientation appears unchanged. Lastly, compared to the SAXS measurements discussed in section 3.2.1 a direct scattering contribution from the confined PEG can be detected down to much smaller pore radii. This is most likely due to the weaker overlaying pore scattering contribution in the WAXS experiments.

References

- 1 C. Appel, M. Kraska, C. Rüttiger, M. Gallei and B. Stühn, *Soft Matter*, 2018, **14**, 4750-4761
- 2 Y. Takahashi and H. Tadokoro, *Macromolecules*, 1973, **6**, 672–675